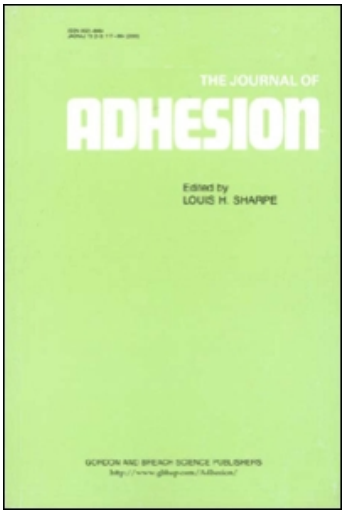

The Journal of Adhesion
Publication details, including instructions for authors and subscription information:
http://www.informaworld.com/smpp/title~content=t713453635

The effect of interphase curing on interphase properties and formation

W. M. Cross[a]; F. Johnson[a]; J. Mathison[a]; C. Griswold[a]; J. J. Kellar[a]; L. Kjerengtroen[b]
[a] Department of Materials and Metallurgical Engineering, South Dakota School of Mines and Technology, Rapid City, South Dakota, USA [b] Department of Mechanical Engineering, South Dakota School of Mines and Technology, Rapid City, South Dakota, USA

Online publication date: 08 September 2010

To cite this Article Cross, W. M. , Johnson, F. , Mathison, J. , Griswold, C. , Kellar, J. J. and Kjerengtroen, L.(2002) 'The effect of interphase curing on interphase properties and formation', The Journal of Adhesion, 78: 7, 571 — 590
To link to this Article: DOI: 10.1080/00218460213736
URL: http://dx.doi.org/10.1080/00218460213736

The Journal of Adhesion, 78: 571–590, 2002

0021-8464/02 $12.00 +.00
DOI: 10.1080/00218460290010296

THE EFFECT OF INTERPHASE CURING ON INTERPHASE PROPERTIES AND FORMATION

W. M. Cross
F. Johnson
J. Mathison
C. Griswold
J. J. Kellar
Department of Materials and Metallurgical Engineering,
South Dakota School of Mines and Technology,
Rapid City, South Dakota, USA

L. Kjerengtroen
Department of Mechanical Engineering,
South Dakota School of Mines and Technology,
Rapid City, South Dakota, USA

Fiber-optic evanescent wave FTIR spectroscopy was combined with phase imaging AFM to examine two thermosetting polymer matrix composite systems. The epoxy/NMA system data from the fiber-optic, evanescent wave FTIR analysis showed incomplete curing (∼75% complete) in the region near the fiber, but essentially complete (∼95% complete) curing in the bulk. Conversely, the unsaturated polyester system exhibited essentially complete curing (∼95% complete) both near the fiber and in the bulk material. For the same samples, phase imaging AFM indicated that the epoxy/NMA system had an ∼2.5 micron thick interphase, while the unsaturated polyester system showed no interphase between the fiber and the matrix. Therefore, the presence of the interphase in the epoxy/NMA system can be attributed to the incomplete curing next to the fiber.

In addition, the systems chosen allowed the reactivity of adsorbed γ-APS coupling agent to be assessed simultaneously with polymer curing. For the epoxy/NMA system, the amine band decreased about 54% during curing. For the polyester system, the amine band decreased 43% during curing.

Received 16 July 2001; in final form 18 January 2002.

This is one of a collection of papers honoring Hatsuo (Ken) Ishida, the recipient in February 2001 of *The Adhesion Society Award for Excellence in Adhesion Science, Sponsored by 3M.*

This work was supported by NSF grants, numbers CMS-9900383 and DMR-9724532.

Address correspondence to Jon J. Kellar, Department of Materials and Metallurgical Engineering, South Dakota School of Mines and Technology, 501 E. St. Joseph St., Rapid City, SD 57701, USA. E-mail: jon.kellar@sdsmt.edu

Keywords: Fiber-optic evanescent wave FTIR spectroscopy; Phase imaging AFM; Epoxy/NMA; Polyester; Interphase

INTRODUCTION

The existence of a transition zone between the reinforcement and matrix in polymer matrix composites (PMCs) has been postulated for over 25 years [1]. In PMCs, this transition zone is often termed the interphase. Only within the last 5–10 years have the techniques become available to allow investigation of the interphase. In particular, various atomic force microscopy (AFM) techniques such as phase imaging and force modulation [2–4], in addition to nanoindentation [5], have shown the existence of the interphase. A variety of causes have been put forth to explain the existence of the interphase, including restraint of polymer movement by the reinforcing material, and alteration of the stoichiometry of the polymer in the viceinity of the reinforcement due to differences in the force of attraction between the polymer components and the reinforcement surface. Recent work by VanLandingham and coworkers [2] gives some evidence for differences in the near-surface stoichiometry. Restriction in polymer movement may possibly be seen in the recent work of Kumar et al. [3], who found a significant fiber effect in nanoindentation measurements.

Ishida and coworkers [5–8] have done considerable work in characterizing the interphase region. In particular, Ishida and coworkers [5–8] examined the different types of bonding of coupling agents adsorbed at reinforcement surfaces. Adsorbed coupling agent can be either physically adsorbed or chemically adsorbed to the surface. The physically adsorbed material is loosely held to the surface through van der Waals bonds, while the chemically adsorbed material is covalently bonded to the surface or covalently bonded to material that is covalently bonded to the surface. The amount of each type of material is highly dependent upon the acid-base nature of the surface, the surface chemistry of the reinforcement, and the amount of silane used. The interphase is then affected by the nature and type of silane at the reinforcement surface. Although the silane is expected to be reactive with the matrix, the inner layers of silane have been shown to be relatively unreactive [9]. The outer layers, particularly the chemisorbed layers, can bond with matrix especially if the matrix interpenetrates the adsorbed layer. A combination of many analytical techniques has been used to arrive at these results. One of the most useful of these techniques has been infrared spectroscopy.

Several researchers have examined the interphase and its stoichiometry [2, 10–15]. The systems studied were primarily epoxy systems cured with amine and some of the interphase differences observed were shown to be due to preferential adsorption of the constituents (for instance amine at carbon surfaces). However, as this preferential adsorption can only span a few molecular layers other thermodynamic forces act over a greater range to obtain the interphase thicknesses measured.

The use of the infrared (IR) portion of the electromagnetic spectrum to investigate polymer curing behavior goes back to the early 1960s [16, 17]. More recently, the advent of Fourier transform infrared (FTIR) techniques has led to significant improvement of the knowledge base in bulk polymer curing, particularly for epoxy polymers. However, investigation of the interphase is much more difficult and has only been accomplished through the use of IR microscopy or evanescent wave sampling techniques. Infrared microscopy has been utilized by Koenig and coworkers [18] to investigate the interphase. This technique worked well except that the sampling distance was approximately 8 μm compared with the typical interphase size of 0.003–3 μm [19], thereby combining the interphase behavior with that of the bulk. Evanescent wave techniques include the use of large (>1 mm in thickness/diameter) attenuated total reflectance (ATR) elements such as germanium or silicon crystals, and small (<0.1 mm) optical fibers. The ATR elements are generally used in the mid-IR region ($4000–400\,cm^{-1}$) [20–23], while optical fibers have been most often used in the near-IR ($12500–4000\,cm^{-1}$) [24–30] or the visible light ($33333–14500\,cm^{-1}$) region [31]. In general, ATR elements must be coated to begin to resemble a reinforcement surface [21, 23], and these elements are much larger than typical reinforcements [20–23]. Most transparent optical fibers are comprised of pure silica, so that, again, the composition is not particularly similar to glass reinforcements [24, 26, 27, 31] and often the size is much larger than that of reinforcing fibers [24–27, 30, 31].

In this work, phase imaging AFM measurements of interphase size and properties in an epoxy and a polyester matrix composite are combined with IR interphase cure monitoring of the same composite samples, using a recently-developed, soda-lime, thin-clad, glass fiber-optic sensor system [32] to develop new insight into the formation of the interphase. The optics associated with the sensor system are discussed later and a schematic detailing the sensor system is shown in Figure 1.

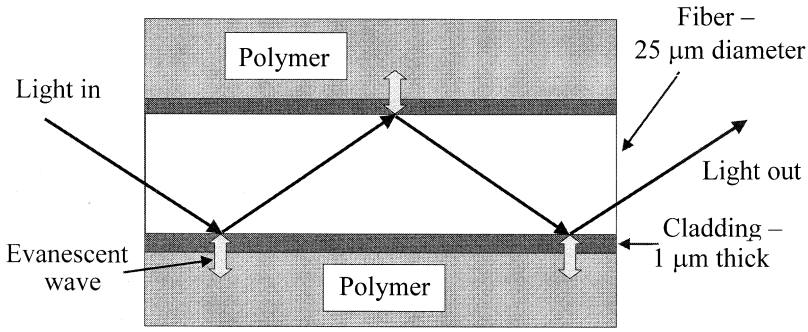

FIGURE 1 Schematic of the fiber-optic evanescent wave FTIR sensing system.

EXPERIMENTAL PROCEDURE

Fiber Optic Cure Monitoring

To obtain the IR spectra necessary for examining the near-fiber curing behavior of the epoxy and polyester polymers investigated, a four-step approach was utilized. First, a group of 300–350 optical fibers ($\sim$25 μm diameter, soda-lime clad, flint-glass core from Dolan-Jenner, Lawrence, MA; Johnson et al. [28, 29, 33] for more information) were bundled together into an SMA 905 connector using a small amount of room temperature curable epoxy (Hysol 608, Applied Products, Inc., Minnetonka, MN). The fiber ends were hand polished in 5 stages from 12 to 0.3 μm using aluminum oxide polishing papers (Fiber Instrument Sales, Inc., Oriskany, NY). The ends were cleaned with isopropyl alcohol between each polishing stage. Second, the sensing region of the fibers was cleaned of contaminants by soaking in Nochromix® for 15 min. The fibers were then rinsed thoroughly in distilled water, connected to the fiber optic accessory (Bio-Rad Digilab), and dried at 190°C (epoxy system) or 120°C (polyester system). The drying temperature was chosen to be the highest temperature achieved during the subsequent polymer curing process. After the fiber bundles were cooled to room temperature, the fibers were separated using a glass stirring rod and a background spectrum was recorded. This spectrum contained 1024 coadded scans obtained at 10 MHz scan speed and resolution 16 cm^{-1} (indicating a point taken every 8 cm^{-1}) over the spectral range 10,000 to 4,000 cm^{-1}. Third, the cleaned fiber bundles were treated at room temperature with a 2 wt% aqueous solution of γ-aminopropyltrimethoxy silane (γ-APS) for 1 h, dried at 100°C for 1 h, and then cooled to room temperature. Following the γ-APS treatment,

a spectrum of the adsorbed silane layer was obtained by coadding 512 scans using the same scan speed, resolution, and spectral range noted above. For those samples that were not to be treated with γ-APS, the fiber bundles were placed in distilled water for 1 h and dried at 100°C for 1 h, so that all bundles underwent as nearly identical treatment as possible. Fourth, polymer was added to the curing cell, and the polymer cured as described in the next section. During curing, spectra of the epoxy system were obtained every 20 min, while spectra were collected every 10 min for the polyester system. All polymer curing spectra were obtained with 512 coadded scans, 10 MHz, 16 cm^{-1}, 10,000–4,000 cm^{-1}. Each spectrum took approximately 4 min to collect so that the data obtained is an average over these 4-min intervals.

All spectra were collected on a Bio-Rad Digilab FTS-40A operating in the near-IR. This spectrometer utilizes a tungsten-halogen light source and quartz beamsplitter. The detector used was part of the fiber optic accessory and was a liquid nitrogen-cooled, wide-band, mercury-cadmium-telluride (MCT) detector. The spectrometer was controlled by Grams/32 based Win-IR software. All spectral manipulations, including baseline correction and quantification, were performed on this workstation. An in-depth discussion of the spectral manipulation procedure can be found in Johnson [33].

Transmission FTIR Spectroscopy

Examination of cured and uncured polymer samples was accomplished using transmission FTIR spectroscopy. For the cured samples, 50–100 μm sections with parallel faces were cut from the same samples for which fiber-optic cure monitoring was performed. Near-IR light (10,000–4,000 cm^{-1}) was passed through the thin samples, and spectra were collected using 256 scans at resolution 8 cm^{-1} and a scan speed of 10 MHz.

The uncured polymer was mixed as described in the polymer curing sections given below. A small amount of the uncured polymer was sandwiched between ZnSe plates and placed in the spectrometer sample compartment. The spectra of the uncured polymer samples were collected using the same parameters as the cured polymer samples described in the previous paragraph. All spectra were collected on a Bio-Rad Digilab FTS-40A operating in the near-IR.

Epoxy Curing

The epoxy used was a commercial bisphenol A, epichlorohydrin resin (Epon 828®, Shell Chemicals, Houston, TX). The curing agent was methyl-5-norbornene-2,3 dicarboxylic acid anhydride (NMA, Sigma

Chemical Co., St. Louis, MA, 9:10 weight ratio with epoxy). In addition, imidazole initiator (Avocado Chemicals, Heysham, UK, 0.5 wt%) was used. The system was cured in a specially designed curing cell equipped with two 150 Watt cartridge heaters (CIR-1014/120 V, Omega Engineering, Inc., Stamford, CT) controlled by a fuzzy logic controller (CN4801-R1, Omega Engineering, Inc., Stamford, CT). A 9:10 weight ratio of curing agent to epoxy was used with 0.5 wt% imidazole initiator. A total of 60 grams of this mixture was poured into the curing cell. The fiber bundle was posi- tioned in the curing cell prior to addition of the mixture, and the curing cell was also heated to 120°C prior to mixture addition. The mixture was cured at 120°C for 1 h; the temperature was raised over a 10-min period to 190°C and held at 190°C for 1 h for the postcure. Following postcure, the cured epoxy was cooled to room temperature and a final spectrum of the cured sample at room temperature was collected.

Polyester Curing

The polyester system used was an unsaturated polyester composed of maleic anhydride, isophthalic acid, and propylene glycol (mole ratio 1:1:2.2) mixed with 45% styrene (Alpha/Owens Corning, E. Collierville, TN). Methyl ethyl ketone peroxide (Sigma Chemical) was used as initiator and cobalt 6% naphthanate (Alfa Aesar, Ward Hill, MA) was the promoter. We added 2.5 wt% of the initiator and 0.24 wt% of the promoter to the unsaturated polyester/styrene resin. Forty grams of this mixture was poured at room temperature over the fibers and into the same curing cell as described in the epoxy curing section. After a 1-h cure at room temperature, the cell was heated to 120°C for a 1-h postcure. This heating took approximately 5 min. Following postcure, the cured polyester was cooled to room temperature and a final spectrum of the cured sample was collected.

Phase Imaging AFM

After curing was completed as described in the previous sections, samples were cut from the cured piece and prepared by wafering and polishing for phase imaging AFM.

Wafering

The sample was cut with a diamond-wafering blade (Isomet Wafering Blade) to obtain two flat surfaces. One surface was used to mount the sample to a stainless steel disc, either 12 mm or 15 mm in diameter. The technique described below was used to polish the parallel surface.

Polishing

MasterTex® polishing cloth was used in conjunction with oil-soluble diamond paste (Buehler MetaDi Polishing Compound). The sample underwent 4 main stages of polishing. Each stage consisted of wet polishing at high and low velocities. The high velocity polish was held for 30 s, whereas each low velocity polish was held for 1 min. The first stage of polishing was performed using 3 μm diamond paste. Next, 1 μm, and then 0.25 μm, diamond paste was used to remove most of the deeper scratches. The fourth stage was conducted using a 0.05 μm alumina suspension. The polishing technique resulted in a surface with a deviation between fiber and matrix of 50 nm to 1 μm.

Once the polishing was completed, surface debris was removed using a sonic bath. The sample was placed in a 50/50 isopropyl alcohol/distilled water solution. It was in the bath for 2 fifteen-min cycles, with approximately 10 min between cycles.

Phase Imaging

Phase imaging was performed using a Digital Instruments Nanoscope IIIa Multi-Mode AFM and a TESP nanoprobe. After the tip was installed in the holder, the laser aligned, sum signal minimized, and the head lowered to the sample, manual tuning was executed. Manual tuning enabled the second drive frequency, ~1.7 MHz, of the cantilever to be exploited. This higher frequency caused the cantilever to have a greater stiffness when compared with its "true" drive frequency of ~300 KHz. Once the second drive frequency was found, a small frequency offset was executed. The offset was used because of the frequency shift, to a lower frequency, caused by dampening effects of sample tip interactions after engagement.

The sample was engaged and scanned with the following parameters: Scan size = 1 μm; Scan rate = 1 Hz; Integral gain = 0.2; Proportional gain = 0.4.

Drive amplitude and setpoint were determined by the software during engagement. A typical value for the drive amplitude was 300 mV, and a typical value for the setpoint was 0.3 V. These values are considerably more when compared with a cantilever that has been tuned to its lower frequency. Once optimal scanning parameters were set, the sample was probed for a suitable region.

RESULTS

Two systems were studied in this work, epoxy/NMA and polyester-styrene. Both systems were examined by a combination of fiber-optic

evanescent wave FTIR spectroscopy and phase imaging AFM, and the results found are given below.

Fiber-Optic Evanescent Wave FTIR

To analyze the data from the fiber-optic evanescent wave FTIR technique, several aspects must be considered. First, the refractive index of the polymer phase is a function of degree of cure [25, 31]. As the amount of material sampled is a function of the refractive index of the outer phase, a method of accounting for the changes due to refractive index variation is necessary. Second, the complexity of the spectra, particularly due to overlapping bands, must be accounted for. Third, the spectroscopic data obtained should be compared with relevant IR data obtained via transmission spectroscopy.

For the refractive index issue, standard attenuated total reflectance (ATR) theory [34–36] can be used as an approximation of fiber-optic theory [37]. For the thin-clad fiber used in this work, the optical fiber needs to be treated as a three-phase system (core/cladding/sample) with an absorbing outer material. The best comparator for the initial and final cure states is the effective path length, b_{eff}, described by Sperline and Freiser [36] from the work of Hansen [34]. The effective path length characterizes the ATR data in terms of an equivalent thickness of a thin film examined by transmission. The relevant equation for b_{eff} is [36]:

$$b_{\text{eff}} = d\langle E_3\rangle^2 n_3/(n_1\cos(\theta)), \tag{1}$$

where d is the decay constant of the evanescent field in the outer phase, $\langle E_3\rangle^2$ is the electric field strength at the cladding/polymer interface ratioed against the electric field strength at the core/clad-cladding interface [35], n_3 is the real portion of the polymer refractive index , n_1 is the core refractive index, and θ is the angle of incidence of the light at the core/cladding interface. The decay constant takes into account the absorption of IR light by the polymer and the wavelength of light used, and can be found from Hansen [34] as

$$d = \lambda/(4\pi\,\text{Im}(\zeta_3)) \tag{2}$$

and

$$\zeta_3 = ((n_3 + ik_3)^2 - (n_1\sin(\theta))^2)^{1/2}, \tag{3}$$

where λ is the wavelength of light and k_3 is the absorptivity of the polymer at λ. The polymer refractive index can be varied, for instance from 1.55 to 1.58, as occurs in epoxy curing [25, 31]. The angle of

incidence can be varied to account for the different modes travelling in the optical fiber. Calculation of b_{eff} from Equation (1) using Equations (2) and (3) indicates that for $k_3 < 0.01$, k_3 has little effect on b_{eff}. As the expected values of k_3 are less than 0.01, k_3 was set to 0.001 for comparison of the b_{eff} values. Second, comparing b_{eff} at $n_3 = 1.55$ and 1.58 and at any incident angle, the ratio of the value of b_{eff} at $n_3 = 1.58$ to $n_3 = 1.55$ was nearly constant, with a value between 2.5 and 3. Thus, the increase of the refractive index due to curing should increase the band heights by about a factor of 3. The refractive index of polyester after curing is approximately the same as that of epoxy given here, so the given analysis should be valid, although the refractive index change during curing was not measured or found in the literature. Finally, the average value of d was calculated to be 0.39 μm. Approximately 98% of the sampling occurs within a distance $2d$ from the cladding/polymer interface. Thus, the overwhelming majority ($> 98\%$) of the signal arises from the first micrometer of polymer adjacent the fiber, making this sensor system ideal for probing the interphase adjacent to a glass fiber.

As was shown in the preceding analysis, the IR band heights will increase by a factor of approximately 3 during curing. Therefore, the more standard method of using band height decrease of a single band will not be effective in measuring the degree of cure. Instead, a different method must be utilized. For this work, the method chosen was to ratio the curing band against a band from a moiety that should be curing-invariant. For both the systems studied, the curing-invariant band used was the phenyl ring stretching-bending combination at 4670–4685 cm^{-1}. The moiety responsible for this band does not participate in the curing reaction and thus should be relatively invariant. With this approach, the results from fiber-optic evanescent wave FTIR examination of the curing behavior of an anhydride cured epoxy and of an unsaturated polyester mixed with styrene were examined.

Epoxy/NMA

Figure 2 shows the spectra of the epoxy/NMA system before and after curing using fiber-optic evanescent wave FTIR spectroscopy. The primary bands of interest occur at $\sim$4530 cm^{-1}, a stretching-bending combination from the CH_2 on the epoxide ring; $\sim$4685 cm^{-1}, a stretching-bending combination of the CH in the phenyl ring; and $\sim$4830 cm^{-1}, which is a band from the NMA [33, 38] and is thought to be due to an overtone of the carbonyl stretching band. For the spectra shown in Figure 2, the band at 4940 cm^{-1} is due to the stretching-bending combination of the terminal NH_2 of the adsorbed silane molecule.

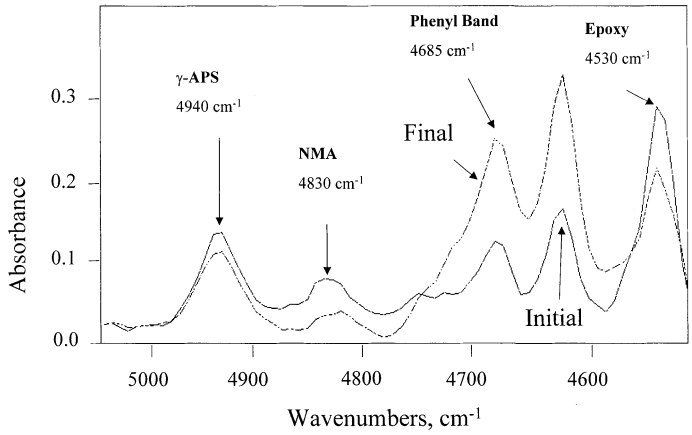

FIGURE 2 Initial and final cure spectra for the epoxy/NMA system.

As can be seen from Figure 2, the phenyl ring band at $\sim 4685\,cm^{-1}$ increases by about a factor of 3 during curing, as predicted from the effective depth calculation. Also, despite the increase expected due to refractive index change, the epoxy ($\sim 4530\,cm^{-1}$), NMA ($\sim 4830\,cm^{-1}$), and γ-APS NH_2 ($\sim 4940\,cm^{-1}$) bands all decrease with cure. To obtain the band heights necessary for examination of the curing behavior, several methods were compared. The details of the comparison are given in Johnson [33], where the best method was found to be a 6-point cubic baseline fit for the epoxy/NMA system over the spectral range 5400 to $4461\,cm^{-1}$. While all the methods tested were subject to user bias, attempts were made to minimize this bias by developing a protocol for the application of each method prior to its utilization.

Figure 3 shows the absorbance ratio ($4830\,cm^{-1}/4685\,cm^{-1}$) versus time graph for the epoxy/NMA system. This graph was obtained by averaging the data from 5 different curing experiments. Examination of the graph in Figure 3 shows that the initial band ratio was 0.405. This initial ratio will be used later for examination of interphase stoichiometry. Also, when the fiber surfaces had been treated with γ-APS, the $4830\,cm^{-1}$ band did not begin to decrease until more than 40 min had passed. This is quite different from the interphase curing behavior in the absence of γ-APS and the bulk epoxy/NMA curing behavior [39], in which curing began essentially immediately. In addition to the NMA band, the curing behavior of the epoxy band was followed. For this band, the onset of curing was, once again, delayed by approximately 40 min (the same as the NMA band) when silane was present. In comparison, curing of NMA in the interphase was delayed

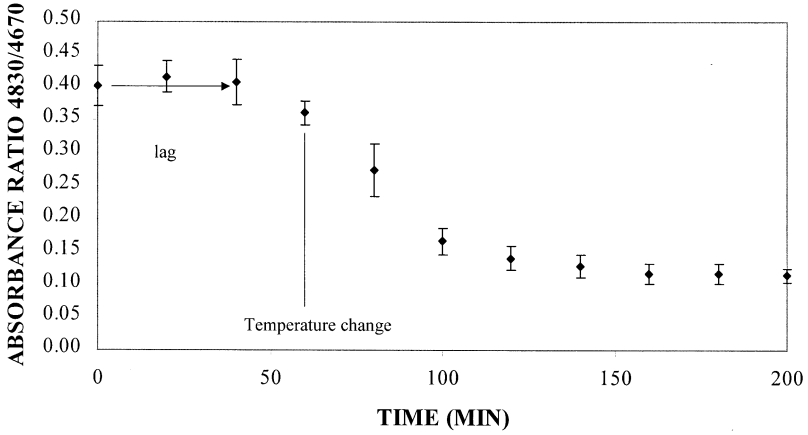

FIGURE 3 Curing as a function of time followed through the 4830 cm^{-1} NMA absorbance band.

approximately 20 min when no adsorbed silane was present and was not delayed in the bulk, according to the work of Antoon and Koenig [39]. Finally, the amine band of the silane began reaction immediately. These data are given in Table 1. The data in Table 1 are the average of 2 separate tests (bulk and no silane) or 5 separate tests (with silane).

Also shown in Table 1 are the final amounts of the bands reacted (labeled "Cure"). Examination of the cure data indicates that, for the NMA band, the amount of the band reacted is not significantly different in any of the situations studied, and that approximately 70–80% of the NMA reacted. These data are in agreement with the bulk data of Antoon and Koenig [39] who showed, using mid-IR analysis, that about a 73% reduction of the NMA band occurred under similar conditions. For the epoxy band, the degree of cure data are significantly different in nature from the NMA data. In particular, the bulk data indicate

TABLE 1 Percent Cure and Lag Time for the Epoxy/NMA System

	4830/ 4685 (NMA)		4530/ 4685 (epoxy)		4940/4685 (γ-APS)	
Sample	Cure(%)	Lag (min)	Cure(%)	Lag (min)	Cure(%)	Lag (min)
Bulk	75–81	0	95–99	0	—	—
Interphase–no silane	82	0	74	20	—	—
Interphase–2% silane	72	40	68	40	54	0

essentially complete reaction of the epoxy, while the interphase data indicate approximately 68–74% reaction. Figure 2 also confirms this incomplete curing of the interphase, as both the NMA band and the epoxy band are present in the final spectrum. The bulk data given for the degree of cure were found by cutting thin sections ($\sim$50–100 μm thick) from samples whose interphase curing was measured by fiber optic evanescent wave FTIR spectroscopy. Thus, these bulk data are directly comparable with the interphase data.

This work can also be compared with the work of Garton [23], in which the curing of an epoxy/NMA system near germanium ATR crystals with various coatings (no coating, aramid fibers, and carbon black) was examined. Curing the epoxy system at both bare germanium and aramid-fiber-coated germanium surfaces resulted in about 80% anhydride reaction, with slightly more curing in the aramid system. These values are quite similar to the values found here (see Table 1), although a different initiator was used. Garton's work [23] also indicated that the amount of adsorbed water played a role in the final amount of anhydride reacted, and this may account for the differences between Garton's work [23] and this work. Finally, in Garton's work [23], no time lag for curing was observed.

The amine band of the γ-APS was also examined for degree of cure. As Figure 2 shows, this band does not disappear completely upon completion of curing. From Table 1, the band height decrease is approximately 54%, which is much greater than the amount of decrease (22%) observed by Connell et al. [27] for γ-APS adsorbed at a silica fiber reacting with EPO-TEK 328®, a fluorinated epoxy monomer. In the case of Connell et al. [27], the decrease was solely attributable to amine reaction, as loss of the adsorbed coupling agent from the surface was tracked through the silane's aliphatic CH overtone bands, and no loss was observed. Thus, the coupling agent did not dissolve into the polymer or expand appreciably due to interpenetration by the polymer. In the present case, this type of tracking could not be performed due to band overlap from the polymer system.

In addition, the reactivity of the amine group can be altered by the presence of adsorbed carbon dioxide and water. Unfortunately, the current experimental procedure does not allow examination of the adsorbed APS layer to determine the extent of amine interaction with these other adsorbed species.

Stoichiometry

To assess the stoichiometry of the epoxy/NMA system, the initial band height ratios for the epoxy ($4530\,cm^{-1}/4685\,cm^{-1}$) and NMA ($4830\,cm^{-1}/4685\,cm^{-1}$) were determined from the fiber-optic evanes-

cent wave FTIR spectra and compared with the same band ratios for bulk samples found by liquid transmission FTIR measurements. This comparison is shown in Table 2. For the interphase data, the value in parentheses is the value calculated from the IR spectra. However, this value must be corrected for the difference in effective depth (b_{eff}, Equation (1)) between the functional group ($4530\,\text{cm}^{-1}$, $4830\,\text{cm}^{-1}$) and the reference band ($4685\,\text{cm}^{-1}$). The corrected value is shown without parentheses in Table 2. Examination of Table 2 shows that, for the no silane experiments, the band ratios are slightly greater—4% for the epoxy band and 8% for the NMA band near the fiber—than in the bulk material. Thus, the near-surface stoichiometry is not greatly different from the bulk stoichiometry, when the glass fibers had no surface treatment. In this case, near-surface indicates the exponentially-weighted average over the distance $2d$ (Equation (2)), about the first 750 nm away from the glass fiber surface.

When the glass fibers were treated with a 2% γ-APS solution, different behavior was observed. With this surface treatment, the epoxy band decreases slightly ($\sim$1%) from the no silane case and is therefore essentially equal to the bulk value. The NMA band, however, decreases considerably, $\sim$30%, for the interphase with silane present, compared with the bulk value. Therefore, with adsorbed silane present the interphase region has considerably less NMA than the bulk polymer. The epoxy content does not appear to change; however, this may be due to the reference band being primarily due to the epoxy, causing the $4530\,\text{cm}^{-1}/4685\,\text{cm}^{-1}$ ratio to be essentially constant because both bands arise from the same species.

In summary, in the interphase with no silane treatment, the ratio of NMA to epoxy is near the bulk value. However, with adsorbed silane the ratio of NMA to epoxy decreases to about 70% of the bulk value. Thus, interphase curing with silane present should be different, from both interphase curing in the absence of silane and bulk curing, due to the stoichiometry change. As was discussed previously, differences in interphase curing were observed with and without silane. The main difference was that with silane present the reaction of the NMA and epoxy ring did not begin until about 40 min after the components were

TABLE 2 Stoichiometry of the Epoxy/NMA System

Sample	4830/4685 (NMA)	4530/4685 (epoxy)
Bulk	0.611	2.615
Interphase–no silane	0.655 (0.635)	2.71 (2.80)
Interphase–2% silane	0.418 (0.405)	2.57 (2.65)

mixed. This may be due to the lack of NMA in the interphase, but one would expect that the NMA reaction and the epoxy reaction would not track each other due to their relative concentration in the interphase. Two possibilities to explain this are (1) that the time scale (~ 4 min) over which each spectrum is collected causes any differences to be obscured, or (2) the delay in ring opening may be due to a decrease in the amount of imidazole initiator in the interphase. Unfortunately, the presence of imidazole could not be traced due to the low levels (0.5 wt%) of imidazole used in the curing. The stoichiometric differences observed do not, however, seem to affect the degree of cure of the polymer.

Polyester

The fiber-optic evanescent wave sensing system was also used to measure the near-fiber curing behavior of an unsaturated polyester/styrene mixture. Figure 4 shows the spectra of the mixture before and after curing. In Figure 4 the primary bands present are due to the styrene and not to the polyester components. The polyester components, isophthalic acid and maleic anhydride, both have their most intense band at approximately 4690 cm^{-1} [33], probably due to the double bond combination similar to the 4685 cm^{-1} band in the epoxy system. Smaller bands for the polyester occur at 4570 cm^{-1} for the isophthalic acid and 4780 cm^{-1} for the maleic anhydride. These bands can be seen mainly as shoulders, although the 4780 cm^{-1} band

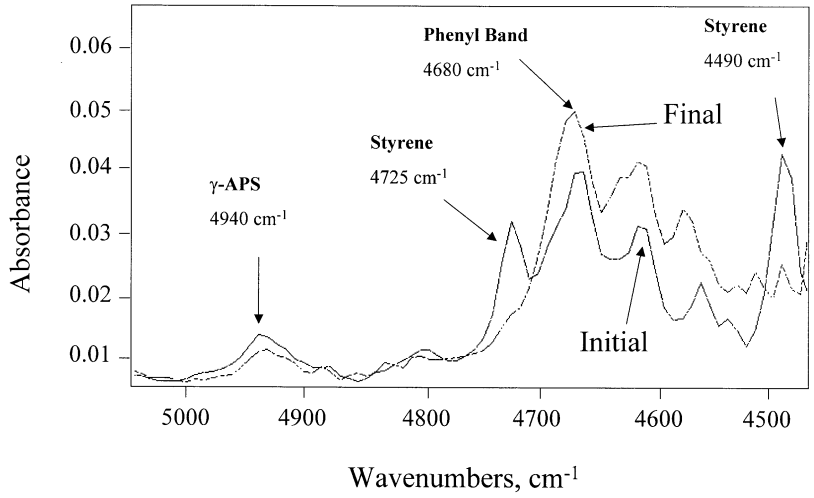

FIGURE 4 Initial and final cure spectra for the polyester system.

for the maleic anhydride is somewhat separated and may be cure sensitive. This is most likely a similar band to the 4830 cm^{-1} band in the NMA, the position difference being due to the different substitutions on the anhydride (C=C for the maleic and the ring structure for the NMA). The styrene is expected to predominate in the spectra because the molar ratio of styrene to maleic anhydride (or isophthalic acid) is 3.4:1. Thus, there are nearly 3.5 moles of styrene for every mole of maleic anhydride (or isophthalic acid). The mole ratio of styrene to propylene glycol is about 1.5:1, but propylene glycol has no absorbance bands in the region studied [33]. As the isophthalic acid and maleic anhydride bands are generally small shoulder bands, these bands have not been examined in the current work but will be studied in a future work.

To examine the reactivity of the polyester system, particularly of the styrene, the same baseline fit procedure as in the epoxy/NMA system was used. The heights of the reactive styrene bands at 4725 and 4490 cm^{-1}, along with the nonreactive band at 4680 cm^{-1}, were determined as a function of time of reaction. Similar to the epoxy/NMA system, the band ratios of the reactive bands to the nonreactive band were used to overcome the effects of the changing refractive index and temperature. The recommended cure cycle for this system was 1 h curing at room temperature followed by 1 h at 120°C postcure. Table 3 shows the degree of cure data for the polyester system's styrene bands. As Figure 4 and Table 3 show, an adsorbed aminosilane (γ-APS) was used. The silane was adsorbed to the fiber sensors from a 2 wt% solution in water. Other silanes were tried, but both γ-methacryloxypropyltrimethoxysilane (MPS, Sigma Chemical) and N-2-aminoethyl-3-aminopropyltrimethoxysilane (AAPS, Petrarch Systems) were not observed in the IR spectra. MPS was not observed, most likely because its main IR band was covered by the styrene

TABLE 3 Percent Cure and Lag Time for the Polyester System

	4725/4680 (styrene)		4490/4680 (styrene)		4940/4680 (γ-APS)	
Sample	Cure (%)	Lag (min)	Cure (%)	Lag (min)	Cure (%)	Lag (min)
Bulk	~95	0	95–99	0	—	—
Interphase–no silane	~95 (29%—1 h)	10	~95 (31%—1 h)	10	—	—
Interphase–2% silane	~95 (26%—1 h)	0	~95 (40%—1 h)	0	43 (24%—1 h)	0

double bond band at 4725 cm^{-1}. AAPS was not observed because its spectrum is much weaker than γ-APS. The γ-APS amine band at 4940 cm^{-1} decreased 24% during the first hour and 43% overall. The overall decrease is less than the decrease in the epoxy/NMA system (54%). Less decrease was expected as γ-APS is not known to be particularly reactive with polyester. Once again, the aliphatic CH overtone bands of γ-APS could not be observed in this system; therefore, diffusion of the coupling agent from the surface could not be differentiated from reaction of the coupling agent.

From Table 3, the bulk styrene band ratios decreased by about 95%, indicating that styrene curing was nearly complete after the entire curing cycle. For the interphase, after 1 h at room temperature the bands had decreased by about 30% with no significant difference either with or without silane. In the absence of silane, the styrene takes 10 min to begin reacting, while reaction begins essentially instantaneously with silane present. Thus, the aminosilane may cause an increase in the amounts of initiator and/or promoter in the interphase region or promote double bond breakage itself, thereby causing the reaction to begin sooner in the sampled region. When the temperature was raised to 120°C the double bond bands disappeared completely from the IR spectra. Because of the speed of disappearance, only the final decrease of the band ratios could be measured. This final decrease for styrene is about 95%, which is essentially the same as the decrease in the bulk band ratio. This is fundamentally different from the behavior of the epoxy/NMA system, in which the reacting interphase bands, particularly for the epoxy bands, were only about 75–80% reacted at full cure. The stoichiometry was not investigated for the polyester system because all bands followed were from the styrene, and hence no stoichiometric information could be determined.

Phase Imaging AFM

The fully cured, fiber-optic evanescent wave FTIR spectroscopy samples were cut and polished as described in the experimental procedure section and then examined by phase imaging AFM. Phase imaging AFM utilizes an oscillating cantilever. The phase lag of the cantilever oscillation with respect to the signal sent to the cantilever is measured. This phase lag is sensitive to material property variation with a stiffer region appearing brighter in the phase image [40], although adhesion and viscoelasticity also affect the phase image signal [41]. Figures 5 and 6 show representative phase images for the epoxy/NMA and unsaturated polyester systems, respectively. The images in both of these figures were obtained from the samples containing silane, as

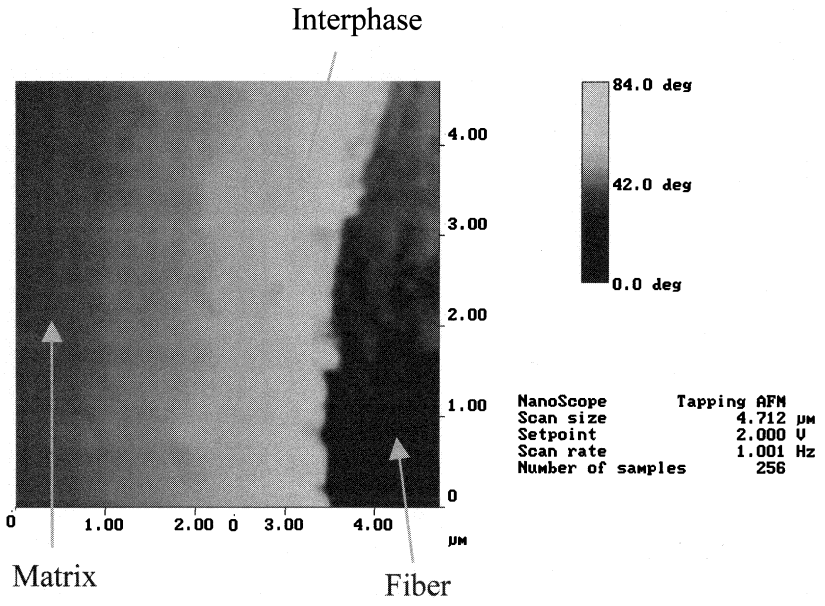

FIGURE 5 Phase imaging AFM view of the epoxy/NMA system near a fiber (see Color Plate I).

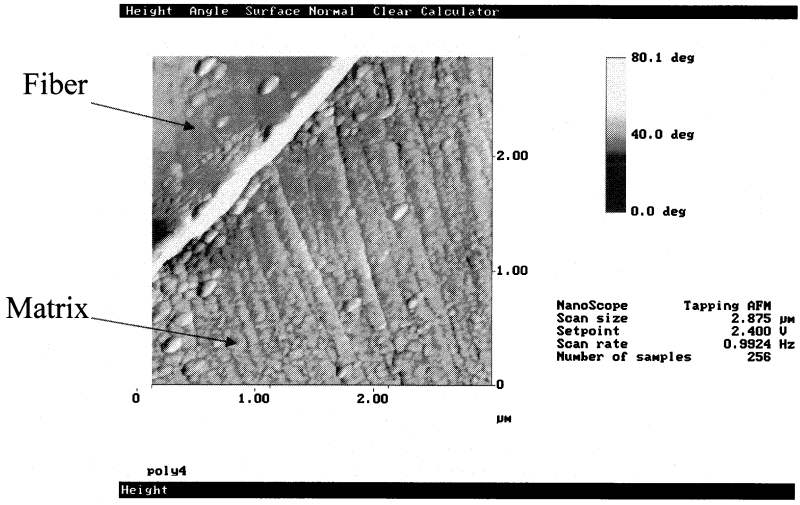

FIGURE 6 Phase imaging AFM view of the polyester system near a fiber (see Color Plate II).

the samples without silane separated at the fiber/matrix interface during sample preparation so that no phase images could be obtained. In Figure 5, a region of differing phase exists between the matrix and fiber. This region is taken to be the interphase. This interphase region appears to extend about 2.5 micrometers from the fiber surface, including a transition of the phase lag to that of the matrix occurring over about the last micrometer. An in-depth phase imaging AFM investigation of the interphase in the same epoxy/NMA system revealed an interphase of between 2.4 and 2.9 μm, invariant of silane treatment [19]. In Figure 6, a representative phase image from the unsaturated polyester system is shown. In this image, the white region at the edge of the fiber is an artifact from the fiber, not an interphase. Examination of Figure 6 shows essentially no transition region between the matrix and the fiber, and hence no interphase region.

DISCUSSION

The epoxy/NMA system data from the fiber-optic evanescent wave FTIR showed incomplete curing (~75% complete) in the region near the fiber but essentially complete (~95% complete) curing in the bulk. Conversely, the unsaturated polyester system exhibited essentially complete curing of the styrene (~95% complete) both near the fiber and in the bulk material. For the same samples, phase imaging AFM indicated that the epoxy/NMA system had an ~2.5 micrometer thick interphase, while the unsaturated polyester system showed no interphase between the fiber and the matrix.

Therefore, the results found in this work suggest that the interphase region in the epoxy/NMA system forms due to incomplete curing of the matrix in the vicinity of the fiber. The presence of silane (γ-APS) alters the stoichiometry in the interphase and causes the onset of the reaction of the epoxy and NMA to be delayed but does not appreciably change the final amount reacted. Thus, both the interphase stoichiometry and the presence of silane do not seem to have much effect on interphase properties as measured by phase imaging AFM. Thus, the more conventional route of making samples of different stoichiometries (see, for instance, Vanlandingham et al. [2]) and measuring the tensile properties may not be of use for identifying the interphase material properties. Instead, other routes must be taken to determine the interphase material properties. Some other possible routes include direct measurement through the phase lag response [41] and nanoindentation [2–4], although both of these routes have problems that would need to be overcome. The phase lag response is a function of both the material properties (Young's modulus and Pois-

son's ratio) and the adhesion energy. The effect of the incomplete curing on the adhesion energy must be known before the material properties can be found. Nanoindentation response is highly dependent upon the load. In particular, very low loads ($< 1-10\,\mu N$) are necessary to limit the volume of material affected by the indentation so that the differences between the bulk polymer matrix and the interphase can be seen [2]. In addition, the low loads are necessary to prevent biasing of the indentation data by the nearby presence of the much stiffer fiber [3].

CONCLUSION

Fiber-optic evanescent wave FTIR spectroscopy was combined with phase imaging AFM to examine two thermosetting polymer matrix composite systems, epoxy/NMA and polyester/styrene copolymer, an unsaturated polyester composed of maleic anhydride, isophthalic acid and propylene glycol mixed with 45% styrene. Phase imaging AFM indicated that the epoxy/NMA system exhibited an ~ 2.5 micrometer thick interphase region, while the polyester system showed little or no interphase region. The spectroscopic results indicated that the epoxy/NMA system did not fully cure near the sensing glass fibers, while the polyester system was fully cured adjacent to the sensing fiber. For both systems, the bulk polymer was shown to be fully cured. Therefore, the presence of the interphase in the epoxy/NMA system can be attributed to the incomplete curing next to the fiber.

In addition, the systems chosen allowed the reactivity of adsorbed γ-APS coupling agent to be assessed simultaneously with polymer curing. For the epoxy/NMA system, the amine band decreased about 54% during curing. This is considerably more than the amount of decrease seen previously in a different epoxy system. For the polyester system, the amine band decreased 43% during curing.

These results show the first correlation between the curing near a fiber in a polymer matrix composite and the interphase region produced in that composite material.

REFERENCES

[1] Sharpe, L. H., *J. Adhesion* **4**, 51 (1972).
[2] Vanlandingham, M. R., Eduljee, R. F., and Gillespie, Jr., J. W., *J. Appl. Polym. Sci.* **71**, 699 (1999).
[3] Kumar, R., Cross, W. M., Kjerengtroen, L., and Kellar, J. J., accepted for publication in *Composite Interfaces* (2002).
[4] Kim, J.-Y., Sham., M.-L., and Wu, J. C., *Composites Part A* **32A**, 607 (2001).
[5] Ishida, H., *Polym. Comp.* **5**, 101 (1984).

[6] Ishida, H., *Polym. Sci. Tech.* **27**, 25 (1985).
[7] Ishida, H., and Miller, J. D., *Macromolecules* **17**, 1659 (1984).
[8] Graf, R. T., Koenig, J. L., and Ishida, H., *J. Adhesion* **16**, 97 (1983).
[9] Rothon, R., *Particulate-Filled Polymer Composites* (Longman Scientific & Technical, Harlow UK, 1995), p. 148.
[10] Chiang, C.-H., and Koenig, J. L., *J. Polym. Sci., Polym. Phys. Edn*. **20**, 2135 (1980).
[11] Drzal, L. T., *Vacuum* **41**, 1615 (1990).
[12] Al-Moussawi, H., Drown, G. K., and Drzal, L. T., *Polym. Comp*. **14**, 195 (1993).
[13] Palmese, G. R., Ph. D. Dissertation, University of Delaware (1992).
[14] Palmese, G. R., McCullough, R. L., and Sottos, N. R., *J. Adhesion* **52**, 101 (1995).
[15] Tanoglu, M., Ziaee, S., McKnight, S. H., Palmese, G. R., and Gillespie, Jr., J. W., *J. Mater. Sci*. **36**, 3041 (2001).
[16] Dannenberg, H., *SPE Transactions* **78** (1963).
[17] Goddu, R. F., and Delker, D. A., *Anal. Chem*. **32**, 140 (1960).
[18] Arvanitopoulos C. D., and Koenig, J. L., *Appl. Spec*. **50**, 1 (1996).
[19] Downing, T., Kumar, R., Cross, W., Kjerengtroen, L., and Kellar, J., *J. Adhes. Sci. Tech*. **14**, 1801 (2000).
[20] Xu, L., and Schlup, J. R., *Appl. Spec*. **50**, 109 (1996).
[21] Garton, A., and Daly, J. H., *Polym. Comp*. **6**, 195 (1995).
[22] Skourlis, T. P., and McCullough, R. L., *J. Appl. Polym. Sci*. **52**, 1241 (1994).
[23] Garton, A., *Infrared Spectroscopy of Polymer Blends, Composites and Surfaces* (Hanser Publishing, New York, 1992).
[24] George, G., Cole-Clarke, P., St. John, N., and Friend, G., *J. Appl. Polym. Sci*. **42**, 643 (1991).
[25] Powell, G. R., Crosby, P. A., Waters, D. N., France, C. M., Spooncer, R. C., and Fernando, G. F., *Smart Mater. Struct*. **7**, 557 (1998).
[26] Cossins, S., Connell, M., Cross, B., Winter, R., and Kellar, J., *Appl. Spec*. **50**, 900 (1996).
[27] Connell, M., Cross, W., Snyder, T., Winter, R., and Kellar, J., *Composites Part A* **29A**, 495 (1998).
[28] Johnson, F., Cross, W., Boyles, D., and Kellar, J., *Composites Part A* **31A**, 959 (2000).
[29] Johnson, F., Connell, M., Duke, E., Cross, W., and Kellar, J., *Appl. Spec*. **52**, 1126 (1998).
[30] Dunkers, J. P., Flynn, K. M., Huang, M. T., and McDonough, W. G., *Appl. Spec*. **52**, 552 (1998).
[31] Afromowitz, M., and Lam, K., *Appl. Optics* **34**, 5635 (1995).
[32] Kellar, J. J., Cross, W. M., Johnson, F. J., and Connell, M. E., U. S. Patent Number 6,198,861, 6 March 2001.
[33] Johnson, F., M. S. Thesis, South Dakota School of Mines and Technology (2000).
[34] Hansen, W. N., *J. Opt. Soc. Am*. **58**, 380 (1968).
[35] Mirabella, Jr., F. M., and Harrick, N. J., *Internal Reflection Spectroscopy: Review and Supplement* (Harrick Scientific, Ossining, NY, 1985).
[36] Sperline, R. P., and Freiser, H., *The Handbook of Surface Imaging and Visualization*, Hubbard, A. T., Ed. (CRC Press, Boca Raton, FL, 1991), Chap. 20, pp. 245–263.
[37] Snyder, A. W., and Love, J. D., *Optical Waveguide Theory* (Chapman-Hall, London, 1983).
[38] Musto, P., Martuscelli, E., Ragosta, G., and Mascia, L., *Polymer* **42**, 5189 (2001).
[39] Antoon, M. K., and Koenig, J. L., *J. Polym. Sci.* **19**, 549 (1981).
[40] Whangbo, W.-H., Magonov, S. N., and Bengel, H., *Probe Microscopy*, **1**, 23 (1997).
[41] Burnham, N. A., Behrend, O. P., Oulevey, F., Gremaud, G., Gallo, P.-J., Gourdon, D., Dupas, E., Kulik, A. J., Pollock, H. M., and Briggs, G. A. D., *Nanotechnol*. **8**, 67 (1997).